AIP Advances

Deposition and spin polarization study of Fe_4N thin films with (111) orientation

Cite as: AIP Advances **7**, 095001 (2017); https://doi.org/10.1063/1.4991963
Submitted: 24 June 2017 . Accepted: 13 August 2017 . Published Online: 01 September 2017

Xuan Li, M. S. Osofsky, Kevin L. Jensen, Hongshi Li, and Jian-Ping Wang

Deposition and spin polarization study of Fe_4N thin films with (111) orientation

Xuan Li,[1] M. S. Osofsky,[2] Kevin L. Jensen,[2] Hongshi Li,[3] and Jian-Ping Wang[1,3,a]

[1]*Department of Electrical and Computer Engineering and the Center for Micromagnetics and Information Technologies (MINT), University of Minnesota, 200 Union St SE, Minneapolis, Minnesota 55455, USA*

[2]*Naval Research Laboratory, 4555 Overlook Ave SW, Washington, DC 20375, USA*

[3]*Department of Chemical Engineering and Materials Science, University of Minnesota, Minneapolis, Minnesota 55455, United States*

(Received 24 June 2017; accepted 13 August 2017; published online 1 September 2017)

We have successfully deposited Fe_4N thin films with (111) out-of-plane orientation on thermally oxidized Si substrates using a facing-target-sputtering system. A Ta/Ru composite buffer layer was adopted to improve the (111) orientation of the Fe_4N thin films. The N_2 partial pressure and substrate temperature during sputtering were optimized to promote the formation of the Fe_4N phase. Furthermore, we measured the transport spin polarization of (111) oriented Fe_4N by the point contact Andreev reflection (PCAR) technique. The spin polarization ratio was determined to be 0.50 using a modified BTK model. The film thickness dependence of the spin polarization was also investigated. The spin polarization of Fe_4N measured by PCAR does not show degradation as the sample thickness was reduced to 10nm. [http://dx.doi.org/10.1063/1.4991963]

I. INTRODUCTION

Ferromagnetic materials with large spin polarization are of great interest for improving the tunneling/giant magnetoresistance ratio of spintronic devices. The γ'-Fe_4N has been theoretically predicted to have a large spin polarization of the density of states at the Fermi level and thus a highly spin-polarized electrical conductance.[1] Extensive studies have been performed on the magnetic and transport properties of Fe_4N after this report.[2–12] The spin polarization of Fe_4N has been experimentally confirmed by point contact Andreev reflection (PCAR) on a (100) oriented Fe_4N thin film.[2] Magnetic tunnel junctions (MTJ) with Fe_4N ferromagnetic electrodes has been reported and their MR ratios are as large as 75% at room temperature.[3,4] Furthermore, unlike the conventional ferromagnetic electrodes such as CoFeB and CoFe, Fe_4N has also been predicted and experimentally proved to be a negative spin polarized material.[5–7] This characteristic provides a pathway for some novel spin-logic devices.[8,9]

To date, most of the spintronics related studies on Fe_4N are based on epitaxial or polycrystalline thin films with (100) out-of-plane orientation.[2,10–12] It is worthwhile to explore Fe_4N films with other orientations for the purpose of multilayer stack integration. For example, the (111) crystal plane is preferred by the exchange bias materials for tunneling/giant magnetoresistive (TMR/GMR) devices.[13] To improve its flexibility for applications, it is also of interest to deposit Fe_4N on the non-magnetic metal buffer layers rather than single crystal substrates, as the metal layers underneath Fe_4N may facilitate a variety of spintronics devices.[3,4,14,15] In addition, the spin polarization of a material is closely related to its growth conditions and crystallinity. Therefore, studying the spin

[a]Author to whom correspondence should be addressed: jpwang@umn.edu

polarization of Fe_4N grown on a practical metal buffer layer is also very helpful for its applications in spintronics.

In this work, we have deposited polycrystalline Fe_4N thin films on thermally oxidized Si substrates. Strong (111) out-of-plane orientation was induced by a Ta/Ru composite buffer layer. The Ta/Ru buffer layer also potentially works as the bottom electrodes of the MTJ/GMR[3,4] and the non-magnetic materials in the spin pumping devices.[14] The nitrogen compositions of the films and the deposition temperature were tuned to optimize the phase formation of Fe_4N. Moreover, the spin polarization of the (111) oriented Fe_4N was measured by the point contact Andreev reflection (PACR) method.[16] The thickness dependence of the spin polarization was also studied.

II. EXPERIMENT

Fe_4N multilayer stacks with a structure of Si thermal oxide/Ta(2nm)/Ru(18nm)/Fe_4N(40nm) were deposited by a DC target-facing-target sputtering system. The base pressure of the sputtering chamber was lower than 6.0×10^{-8}Torr. During the multilayer stack preparation, the Ta/Ru composite buffer layer was first grown on the thermally oxidized Si substrate at room temperature. After that, the Fe_4N layer was deposited by DC reactive sputtering at different substrate temperatures, i.e., 120, 150, 200 and 250°C. To obtain near stoichiometric Fe_4N thin films, the N_2 partial pressure varied from 0.5 mTorr to 1.0 mTorr while the Ar working gas pressure was maintained at 10 mTorr.

The Fe_4N phase and out-of-plane orientations were detected by θ-2θ X-ray diffraction (XRD) using Simens Bruker D5005 with Cu Kα radiation. X-ray photoelectron spectroscopy (XPS) was measured by a Surface Science SSX-100 system to further characterize the compositions and the binding energies of the Fe_4N thin films. Magnetic properties of the samples were examined by a Princeton Measurements vibrating sample magnetometer (VSM). The surface roughness was characterized by an Agilent 5500 atomic force microscope (AFM). We also measured the spin polarization of the (111) oriented Fe_4N by the PCAR technique. The PCAR experimental curves were fitted by a modified[17] Blonder-Tinkham-Klapwijk (BTK) model[18] with fitting parameters spin polarization P and barrier strength Z.

III. RESULTS AND DISCUSSION

Figure 1 shows the out-of-plane X-ray diffraction (XRD) patterns of Fe-N thin films deposited on Ta/Ru buffer layers. A strong hcp-Ru (2000) diffraction signal can be observed in the θ-2θ XRD results. Since Ru does not match with either Ta or Si for their in-plane lattices, the growth mode of the Ru buffer layer is expected to be fiber-textured instead of epitaxial. This was confirmed by the XRD in-plane φ scan, in which no diffraction peak was observed for the Ru due to various lattice rotations in the in-plane direction. The γ'-Fe_4N has the face-centered-cubic Fe lattice with a N atom located at the body center. The in-plane lattice constants of (111) oriented Fe_4N and (1000) Ru are

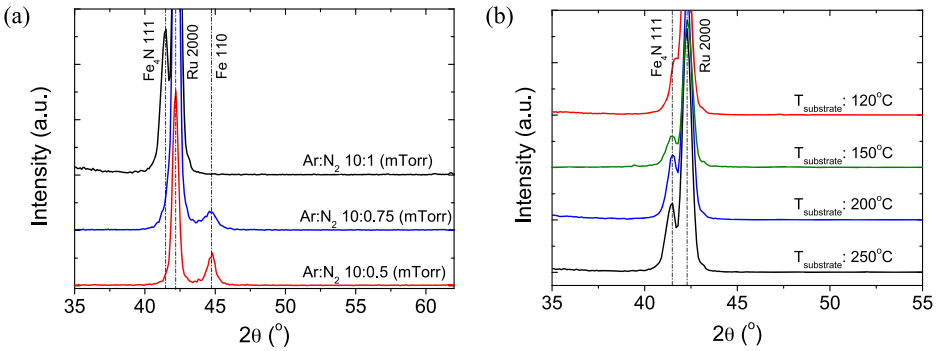

FIG. 1. Out-of-plane X-ray diffraction patterns of 40nm Fe_4N thin films deposited with (a) different N_2 partial pressures; (b) different substrate temperatures.

2.68Å ($a_{Fe4N}/\sqrt{2}$) and 2.69Å (a_{Ru}) respectively, with only a 0.4% lattice mismatch between the Fe_4N {111} and Ru {1000} planes. Therefore, the Ta/Ru buffer layer can facilitate the deposition of (111) oriented Fe_4N. Followed by the growth mode of the Ta/Ru buffer layer, the (111) Fe_4N thin film is also fiber-textured.

Based on the Fe-N phase diagram, several iron nitride compounds can be formed with different Fe:N compositions and temperatures, thus the N_2 partial pressure and substrate temperature need to be controlled in the deposition processes. Figure 1(a) shows the out-of-plane XRD patterns of Fe-N thin films deposited with different N_2 partial pressures. The substrate temperature was maintained at 250°C for all the conditions in Figure 1(a). When the N_2 partial pressure was 0.5 mTorr, the Fe (110) diffraction peak was present in the XRD result, which indicates that the nitrogen composition was insufficient. As the N_2 partial pressure was increased to 0.75 mTorr, the Fe diffraction peak intensity dropped, and the Fe_4N (111) peak appeared. As the N_2 partial pressure was further increased to 1.0 mTorr, the Fe_4N (111) peak became very pronounced, and the Fe (110) signal entirely disappeared. Diffraction peaks from other iron nitrides, for example Fe_3N near $2\theta = 57.5°$ and 60.8°, were absent. Fine tuning the N_2 partial pressure by ±0.1 mTorr around 1.0 mTorr slightly decreased the Fe_4N (111) peak intensity. In subsequent XPS results, we also observed that the N/Fe atomic ratio was nearly stoichiometric for the 1.0 mTorr N_2 sample. Therefore, the N_2 partial pressure was optimized at 1.0 mTorr for the growth of the Fe_4N thin films.

Figure 1(b) shows the out-of-plane XRD results of Fe_4N deposited at different substrate temperatures. As the temperature was gradually tuned from 120°C to 250°C, the intensity of Fe_4N (111) diffraction peaks increased continuously. The strongest Fe_4N (111) signal was observed on the sample deposited at 250°C. Constrained by the deposition system set-up, the substrate temperature could not be further increased during deposition. Alternatively, we post-annealed the best sample (deposited at 250°C) in a different vacuum chamber. When the annealing temperature was 325°C, no noticeable change was observed in the XRD result. The saturation magnetization (M_s) of the optimized sample was measured to be 1250 emu/cm^3 by vibrating sample magnetometry at room temperature. This result is similar to the M_s of Fe_4N thin films reported by several other experimental works.[10,11,15] It is also consistent with our previous experiment result of Fe_4N.[19] The M_s of Fe_4N obtained in this work shows smaller value than the theoretical calculation results that are in a range of 2.1-2.45 μ_B/Fe atom[20–22] (1410-1650 emu/cm^3) at zero temperature (0K). We attribute the smaller M_s of Fe_4N thin films in our experiment to the thermal excitation on magnetization as well as the defects and grain boundaries of the thin film sample.

To demonstrate the effect of buffer layers on the (111) preferred orientation of Fe_4N, we also substituted the Ru (1000) buffer layer with Pd (111) and Pt (111) layers. Compared to the small lattice mismatch between the Fe_4N {111} and Ru {1000} planes (i.e. 0.4%), the mismatches of Pd {111} and Pt {111} are 3.8% and 4.2% respectively. As shown in Figure 2, with the optimized N_2 partial pressure and substrate temperature, the Fe_4N (111) XRD peaks can barely be detected when

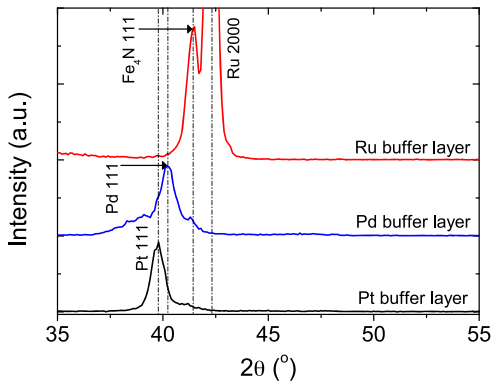

FIG. 2. Out-of-plane X-ray diffraction patterns of 40nm Fe_4N thin films deposited on thermally oxidized Si substrates with Ru, Pd and Pt buffer layers.

the films were deposited on 18nm Pd or Pt layers. In contrast, the sample deposited on the Ru (1000) buffer layer shows a substantially stronger (111) diffraction signal. No Fe_4N peak from the other crystal plane, i.e. (200) at $2\theta = 47.8°$ or (220) at $2\theta = 71.2°$, is observed in the XRD results. Thus, we conclude that the Ru (1000) buffer layer is quite effective for inducing the (111) out-of-plane orientation of Fe_4N.

To further investigate the transport spin polarization of (111) oriented Fe_4N, we performed point contact Andreev reflection (PCAR) measurements on the samples with optimized growth conditions. A superconducting (Nb) tip was gently pressed into the sample to minimize the effect of surface oxidation. At least eight such different contacts were created and tested at a temperature of 1.6K. Figure 3(a) shows normalized conductance $G(V)/G_n$ versus V/V_Δ, in which G_n is the conductance at applied voltage $V >> V_\Delta$ and V_Δ is the superconducting gap of Nb. The PCAR experimental curves were fit by a modified Blonder-Tinkham-Klapwijk (BTK) model with the spin polarization, *P,* and tunnel barrier strength, *Z, as* fitting parameters. The superconducting gap, Δ, was fixed to the value for Nb. For comparison, the same measurement was made on a 40nm Fe (100) sample deposited on a GaAs (100) substrate. The spin polarization was reported as an average of the eight measurements and fits for each sample. It appears that the spin polarization of (111) oriented Fe_4N ($P_{Fe4N} = 0.5$) is statistically larger than that of (100) Fe ($P_{Fe} = 0.44$), as shown in the inset of Figure 3(a). Compared to the Fe_4N deposited on MgO single crystal substrate ($P = 0.59$)[2], our sample shows lower spin polarization which can be partially attributed to the smaller in-plane grain size and the lower degree of crystallinity due to the fiber-textured growth mode of Fe_4N on the Ta/Ru under layer. Also, these samples deposited by sputtering tend to contain more defects than the samples prepared by molecular beam epitaxy (MBE). The defects increase the chance of spin-independent scattering for the electrons thus may also account for the lower spin polarization of our experiment.

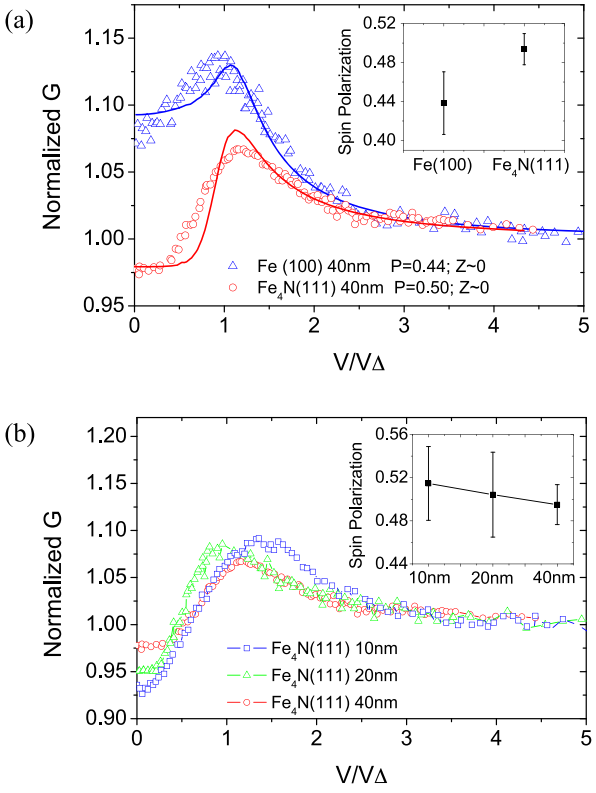

FIG. 3. Point contact Andreev reflection results: Normalized conductance as a function of applied voltage (V) divided by superconducting gap (V_Δ) (a) For (111) oriented Fe_4N and Fe (100); (b) For (111) Fe_4N with different film thicknesses. Experiment data are shown as dots, and fits are shown as continuous curves.

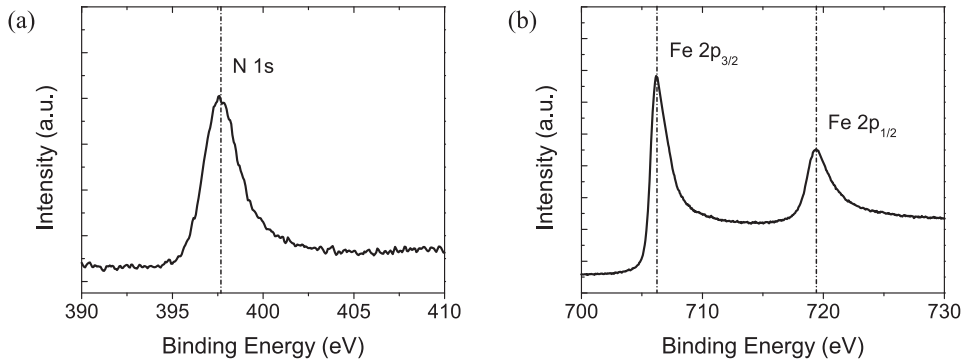

FIG. 4. X-ray photoelectron spectroscopy spectra on (111) Fe_4N sample. (a) Fine scan on N 1s peak; (b) Fe $2p_{3/2}$ and Fe $2p_{1/2}$ peaks.

Although smaller spin polarization was observed, our work does show some advantages compared to the earlier report. First of all, our Fe_4N stack with Ta/Ru under layer is applicable for a group of spintronics devices, for examples MTJ/GMR and spin pumping devices. The spin polarization of Fe_4N in the stack may better represent the properties of Fe_4N in the devices for applications. Furthermore, the Fe_4N film thickness in our report is in a few tens of nanometers, which is closer to the ferromagnetic layer thickness in the spintronics devices. Due to the above two benefits, our spin polarization result of Fe_4N is more practical than the pure material studies. In addition, the spin polarization in this work was reported as a mean of at least eight PCAR measurements for each sample. The averaging of measurements help minimize the testing variations thus make the results more reliable.

In comparison with the theoretical calculations of the spin polarization of Fe_4N,[1,22] both of our study and the earlier experiment report show smaller spin polarization ratios. We attribute the difference between the experiment results and the theoretical calculations to the defects and grain boundaries in the thin film samples, which is normally not considered in the theoretical calculations.

The spin polarization of (111) oriented Fe_4N with different film thicknesses was also studied, as shown in Figure 3(b). The PCAR measurements and fits were performed on the 10nm, 20nm and 40nm (111) Fe_4N thin films. To present the individual measurement curves more clearly, the fits are not shown in this figure. As shown in the inset of Figure 3(b), the (111) oriented Fe_4N samples with smaller thickness (i.e. 10nm, 20nm) do not show a statistical difference from the 40nm Fe_4N sample. On average, the spin polarizations of the three samples are around 0.5 with minor variations. The surface roughness of the 10nm (111) Fe_4N sample was measured by atomic force microscopy, showing a R_a of 0.153nm.

Finally, we performed an X-ray photoelectron spectroscopy (XPS) measurement on the optimized (111) Fe_4N thin film. In Figure 4, Fe 2p3/2, Fe 2p1/2, and N 1s peaks are observed in the XPS result. By calculating the areas under these peaks and normalizing them to their sensitive factors, the N/Fe atomic ratio of 0.22±0.025 is obtained. This result indicates that the optimized (111) Fe_4N sample is close to stoichiometric. In addition, we performed a high resolution scan for the N 1s peak after carbon energy calibration. The N 1s binding energy of the sample was measured to be 397.6eV, which is comparable to the result of another iron nitride $Fe_{16}N_2$.[23]

IV. CONCLUSIONS

In conclusion, (111) oriented Fe_4N thin films have been prepared on thermally oxidized Si wafers by facing-target-sputtering. A Ta/Ru composite buffer layer was used to induce the (111) out-of-plane orientation. The N_2 partial pressure and substrate temperature were optimized to facilitate Fe_4N phase formation. Furthermore, point contact Andreev reflection (PCAR) measurements and fits were performed on the (111) oriented Fe_4N. The transport spin polarization was found to be 0.50, which is larger than that of (100) Fe. The spin polarization of (111) oriented Fe_4N measured by PCAR does not show degradation as the sample thickness approaches 10nm.

ACKNOWLEDGMENTS

This work was partially supported by Seagate Technology. Parts of this work were carried out in the Characterization Facility, University of Minnesota, a member of the NSF-funded Materials Research Facilities Network (www.mrfn.org) via the NSF MRSEC program under award number DMR-0819885. The authors would like to thank Igor Mazin for providing the code to analyze the PCAR measurement data.

[1] S. Kokado, N. Fujima, K. Harigaya, H. Shimizu, and A. Sakuma, Phys. Rev. B **73**, 172410 (2006).
[2] A. Narahara, K. Ito, T. Suemasu, Y. K. Takahashi, A. Ranajikanth, and K. Hono, Appl. Phys. Lett. **94**, 202502 (2009).
[3] K. Sunaga, M. Tsunoda, K. Komagaki, Y. Uehara, and M. Takahashi, J. Appl. Phys. **102**, 013917 (2007).
[4] Y. Komasaki, M. Tsunoda, S. Isogami, and M. Takahashi, J. Appl. Phys. **105**, 07C928 (2009).
[5] K. Ito, K. Okamoto, K. Harada, T. Sanai, K. Toko, S. Ueda, Y. Imai, T. Okuda, K. Miyamoto, A. Kimura, and T. Suemasu, J. Appl. Phys. **112**, 013911 (2012).
[6] M. Tsunoda, Y. Komasaki, S. Kokado, S. Isogami, C. C. Chen, and M. Takahashi, Appl. Phys. Express **2**, 083001 (2009).
[7] K. Ito, K. Kabara, T. Sanai, K. Toko, Y. Imai, M. Tsunoda, and T. Suemasu, J. Appl. Phys. **116**, 053912 (2014).
[8] S. Isogami, M. Tsunoda, Y. Komasaki, A. Sakuma, and M. Takahasi, Appl. Phys. Express **3**, 103002 (2010).
[9] S. Isogami and T. Owada, IEEJ Trans. Electr. Electron. Eng. **9**, S73–S75 (2014).
[10] H. Xiang, F. Y. Shi, M. S. Rzchowski, P. M. Voyles, and Y. A. Chang, J. Appl. Phys. **109**, 07E126 (2011).
[11] W. B. Mi, Z. B. Guo, X. P. Feng, and H. L. Bai, Acta Mater. **61**, 6387 (2013).
[12] Z. R. Li, X. P. Feng, X. C. Wang, and W. B. Mi, Mater. Res. Bull. **65**, 175 (2015).
[13] R. F. C. Farrow, R. F. Marks, S. Gider, A. C. Marley, S. S. P. Parkin, and D. Mauri, J. Appl. Phys. **81**, 4986 (1997).
[14] A. Ruiz-Calaforra, T. Bracher, V. Lauer, P. Pirro, B. Heinz, M. Geilen, A. V. Chumak, A. Conca, B. Leven, and B. Hillebrands, J. Appl. Phys. **117**, 163901 (2015).
[15] S. Isogami, M. Tsunoda, M. Oogane, A. Sakuma, and M. Takahashi, Jpn. J. Appl. Phys. **52**, 073001 (2013).
[16] R. J. Soulen, J. M. Byers, M. S. Osofsky, B. Nadgorny, T. Ambrose, S. F. Cheng, P. R. Broussard, C. T. Tanaka, J. Nowak, J. S. Moodera, A. Barry, and J. M. D. Coey, Science **282**, 85 (1998).
[17] G. T. Woods, R. J. Soulen, I. Mazin, B. Nadgorny, M. S. Osofsky, J. Sanders, H. Srikanth, W. F. Egelhoff, and R. Datla, Phys. Rev. B **70**, 054416 (2004).
[18] G. E. Blonder, M. Tinkham, and T. M. Klapwijk, Phys. Rev. B **25**, 4515 (1982).
[19] Y. Y. Na, C. Wang, J. Z. Xiang, N. A. Ji, and J. P. Wang, J. Cryst. Growth **426**, 117 (2015).
[20] R. Coehoorn, G. H. O. Daalderop, and H. J. F. Jansen, Phys. Rev. B **48**, 3830 (1993).
[21] E. Blanca, J. Desimoni, N. E. Christensen, H. Emmerich, and S. Cottenier, Phys. Status Solidi B **246**, 909 (2009).
[22] Y. Takahashi, Y. Imai, and T. Kumagai, J. Magn. Magn. Mater. **323**, 2941 (2011).
[23] X. W. Zhang, M. Y. Yang, Y. F. Jiang, L. F. Allard, and J. P. Wang, J. Appl. Phys. **115**, 17A767 (2014).